INTERNATIONAL JOURNAL OF
NUMERICAL ANALYSIS AND MODELING
Volume 17, Number 4, Pages 517–531

NUMERICAL INVESTIGATION ON WEAK GALERKIN FINITE ELEMENTS

JUNPING WANG, XIU YE, AND SHANGYOU ZHANG

Abstract. The weak Galerkin (WG) finite element method is an effective and robust numerical technique for the approximate solution of partial differential equations. The essence of the method is the use of weak finite element functions and their weak derivatives computed with a framework that mimics the distribution or generalized functions. Weak functions and their weak derivatives can be constructed by using polynomials of arbitrary degrees; each chosen combination of polynomial subspaces generates a particular set of weak Galerkin finite elements in application to PDE solving. This article explores the computational performance of various weak Galerkin finite elements in terms of stability, convergence, and supercloseness when applied to the model Dirichlet boundary value problem for a second order elliptic equation. The numerical results are illustrated in 31 tables, which serve two purposes: (1) they provide detailed and specific guidance on the numerical performance of a large class of WG elements, and (2) the information shown in the tables may open new research projects for interested researchers as they interpret the results from their own perspectives.

Key words. Weak Galerkin, finite element methods, weak gradient, second-order elliptic problems, stabilizer-free.

1. Introduction

The weak Galerkin (WG) finite element method is an effective and robust numerical technique for the approximate solution of partial differential equations. It is a natural extension of the standard conforming Galerkin finite element method by substituting the classical derivatives with weakly defined discrete derivatives for discontinuous functions. The WG method was first introduced in [17, 18], and since then, it has been applied/extended to several classes of partial differential equations such as biharmonic equations, Stokes equations, Navier-Stokes equations, Brinkman equations, parabolic equations, Helmholtz equation, convection dominant problems, hyperbolic equations, and Maxwell's equations [4, 5, 6, 7, 8, 9, 10, 11, 12, 13, 14, 15, 19].

The main idea of weak Galerkin finite element methods is the use of weak functions and their corresponding weak derivatives. For simplicity, we demonstrate the idea by using the second order elliptic problem that seeks an unknown function u satisfying

$$-\nabla\cdot(\nabla u) = f \quad \text{in } \Omega, \tag{1}$$

$$u = g \quad \text{on } \partial\Omega, \tag{2}$$

where Ω is a polygonal domain in $\mathbb{R}^2$. The primal weak form for the problem (1)-(2) seeks $u \in H^1(\Omega)$ such that $u = g$ on $\partial\Omega$ and satisfying

$$(\nabla u, \nabla v) = (f, v) \quad \forall v \in H_0^1(\Omega). \tag{3}$$

For the variational problem (3), the weak functions possess the form of $v = \{v_0, v_b\}$ with $v = v_0$ inside of each element and $v = v_b$ on the boundary of the element. Both v_0 and v_b can be approximated by polynomials in $P_\ell(T)$ and $P_s(e)$ respectively,

Received by the editors May 2, 2020.
2000 *Mathematics Subject Classification.* 65N15, 65N30, 35J50 .

where T stands for an element and e the edge of T, ℓ and s are non-negative integers with possibly different values. Weak derivatives are defined for weak functions in the sense of distributions. Denote by $G_m(T)$ the vector space for weak gradient. Typical choices for $G_m(T)$ are $[P_m(T)]^d$ or the Raviart-Thomas elements $RT_m(T)$. Each particular combination of $(P_\ell(T), P_s(e), G_m(T))$ leads to a class of weak Galerkin finite element methods tailored for specific partial differential equations.

Weak Galerkin finite element methods have two forms for the problem (1)-(2). The first one is the standard formulation [11, 17] which seeks $u_h \in V_h$ such that $u_h = Q_b g$ on $\partial\Omega$ and satisfying

$$(\nabla_w u_h, \nabla_w v) + s(u_h, v) = (f, v) \quad \forall v \in V_h^0, \tag{4}$$

where $s(\cdot,\cdot)$ is a parameter independent stabilizer. Another one is the stabilizer-free formulation [1, 20, 21]: find $u_h \in V_h$ such that $u_h = Q_b g$ on $\partial\Omega$ and satisfying

$$(\nabla_w u_h, \nabla_w v) = (f, v) \quad \forall v \in V_h^0. \tag{5}$$

Removing the stabilizer from the original WG scheme simplifies the formulation and reduces the programming complexity arising from the stabilizer, but at the cost of increasing the computational complexity for the weak derivative. To have desired stability and convergence, stabilizer-free WG methods must use relatively high values of m for approximating weak gradient in the WG element $(P_\ell(T), P_s(e), G_m(T))$.

The purpose of this paper is to investigate the performance of different WG elements computationally in the weak Galerkin finite element methods with or without stabilizers. The numerical results will be illustrated in 31 tables that are informative and clearly demonstrate special properties of each WG element. It should be noted that not all of the numerical phenomena shown in the tables have theoretical justifications in existing literature; researchers are encouraged to conduct a theoretical investigation for those of their interests.

Table 3 shows that the WG element $(P_k(T), P_k(e), [P_{k+1}]^2)$ has two orders of supercloseness in both energy and L^2 norms on rectangular partitions. Motivated by this computational result, we will provide a theoretical justification for this superconvergence in a forthcoming paper. We note that it has been proved in [2] that the WG element $(P_k(T), P_{k+1}(e), [P_{k+1}]^2)$ has two orders of supercloseness in both energy norm and L^2 norm, on general triangular meshes in Table 18. Furthermore, to overcome the poor performance of the WG element $(P_k(T), P_{k-1}(e), [P_{k+1}]^2)$ shown in Table 24 and 29, a new weak gradient was introduced in [22] so that the element can still converge in optimal order on general polytopal meshes.

The WG methods are designed for discontinuous approximations on general polytopal meshes. Due to limited space, this paper shall only consider the finite element partitions with rectangular and triangular elements.

2. Weak Galerkin Finite Element formulations

Let $\mathcal{T}_h$ be a partition of the domain Ω consisting of rectangles or triangles. Denote by $\mathcal{E}_h$ the set of all edges in $\mathcal{T}_h$, and let $\mathcal{E}_h^0 = \mathcal{E}_h \backslash \partial\Omega$ be the set of all interior edges or flat faces. For every element $T \in \mathcal{T}_h$, we denote by h_T its diameter and mesh size $h = \max_{T\in\mathcal{T}_h} h_T$ for $\mathcal{T}_h$. Let $P_k(T)$ consist all the polynomials defined on T of degree less or equal to k.

Definition 1. *For $T \in \mathcal{T}_h$ and $\ell, s \geq 0$, define a local WG element $W_{\ell,s}(T)$ as,*

$$W_{\ell,s}(T) = \{v = \{v_0, v_b\} : \ v_0|_T \in P_\ell(T),\ v_b|_e \in P_s(e),\ e \subset \partial T\}. \tag{6}$$

Definition 2. *For any $v = \{v_0, v_b\} \in W_{\ell,s}(T)$, a weak gradient $\nabla_w v \in G_m(T)$ is defined as a unique solution of the following equation*

$$(\nabla_w v, \mathbf{q})_T = -(v_0, \nabla \cdot \mathbf{q})_T + \langle v_b, \mathbf{q} \cdot \mathbf{n} \rangle_{\partial T} \qquad \forall \mathbf{q} \in G_m(T). \tag{7}$$

A typical choice of $G_m(T)$ is $[P_m(T)]^d$, or $RT_m(T)$. Different combinations of (ℓ, s, m) associated with a WG element $W_{\ell,s}(T)/G_m(T)$ leads to different weak Galerkin finite element formulations. The weak gradient ∇_w defined in (7) is an approximation of ∇ that is computed on each element T.

Remark 1. *Please note that the space $G_m(T)$ is used to calculated weak gradient and does not introduce additional degrees of freedom to the resulting linear system.*

Definition 3. *Define a WG finite element space V_h associated with $\mathcal{T}_h$ as follows*

$$V_h = \{v = \{v_0, v_b\} : \ \ v|_T \in W_{\ell,s}(T), \ \forall T \in \mathcal{T}_h\}. \tag{8}$$

We would like to emphasize that any function $v \in V_h$ has a single value v_b on each edge $e \in \mathcal{E}_h$. The subspace of V_h consisting of functions with vanishing boundary value is denoted as V_h^0.

Let Q_0 and Q_b be the two element-wise defined L^2 projections onto $P_\ell(T)$ and $P_s(e)$ on each $T \in \mathcal{T}_h$, respectively. Define $Q_h u = \{Q_0 u, Q_b u\} \in V_h$. Let $\mathbb{Q}_h$ be the element-wise defined L^2 projection onto $G_m(T)$ on each element $T \in \mathcal{T}_h$.

For simplicity, we adopt the following notations,

$$\begin{aligned} (v, w)_{\mathcal{T}_h} &= \sum_{T \in \mathcal{T}_h} (v, w)_T = \sum_{T \in \mathcal{T}_h} \int_T vw d\mathbf{x}, \\ \langle v, w \rangle_{\partial \mathcal{T}_h} &= \sum_{T \in \mathcal{T}_h} \langle v, w \rangle_{\partial T} = \sum_{T \in \mathcal{T}_h} \int_{\partial T} vw ds. \end{aligned}$$

Weak Galerkin Algorithm 1. *A numerical approximation for (1)-(2) can be obtained by seeking $u_h = \{u_0, u_b\} \in V_h$ satisfying $u_b = Q_b g$ on $\partial\Omega$ and the following equation:*

$$(\nabla_w u_h, \nabla_w v)_{\mathcal{T}_h} + s(u_h, v) = (f, \ v_0) \quad \forall v = \{v_0, v_b\} \in V_h^0, \tag{9}$$

where the stabilizer $s(\cdot, \cdot)$ is defined as

$$s(u_h, v) = \sum_{T \in \mathcal{T}_h} h_T^j \langle Q_b u_0 - u_b, Q_b v_0 - v_b \rangle_{\partial T}. \tag{10}$$

Let $j = \infty$ in (10), we mean $s(u_h, v) = 0$, i.e., we have the following stabilizer-free WG formulation,

$$(\nabla_w u_h, \nabla_w v)_{\mathcal{T}_h} = (f, \ v_0) \quad \forall v = \{v_0, v_b\} \in V_h^0. \tag{11}$$

In the following sections, we will conduct extensive numerical tests to study the performance of different WG elements and record the results in 31 tables. In all the tables below, $j = \infty$ refers to the stabilizer free WG formulation (11), where j is defined in (10). The element $RT_k(T)$ standards for the Raviart-Thomas element on triangles throughout the paper.

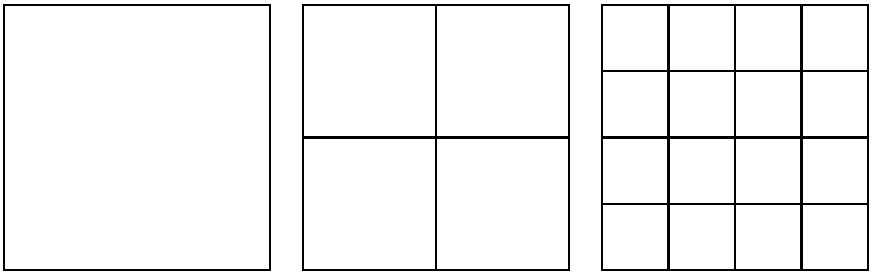

FIGURE 1. The first three level rectangular grids.

TABLE 1. Element $(P_k(T), P_k(e), [P_{k-1}(T)]^2)$ on rectangular mesh, $|||\cdot||| = O(h^{r_1})$ and $\|\cdot\| = O(h^{r_2})$.

element	$P_k(T)$	$P_k(e)$	$[P_{k-1}(T)]^2$	j	r_1	r_2	Proved
1.1				-1	1	2	Yes
1.2				0	0.5	1	No
1.3	$P_1(T)$	$P_1(e)$	$[P_0(T)]^2$	1	0	0	No
1.4				∞	$-\infty$	$-\infty$	No
1.5				-1	2	3	Yes
1.6				0	1.5	2	No
1.7	$P_2(T)$	$P_2(e)$	$[P_1(T)]^2$	1	1	1	No
1.8				∞	$-\infty$	$-\infty$	No
1.9				-1	3	4	Yes
1.10				0	2.5	3	No
1.11	$P_3(T)$	$P_3(e)$	$[P_2(T)]^2$	1	2	2	No
1.12				∞	$-\infty$	$-\infty$	No

TABLE 2. Element $(P_k(T), P_k(e), [P_k(T)]^2)$ on rectangular mesh, $|||\cdot||| = O(h^{r_1})$ and $\|\cdot\| = O(h^{r_2})$.

element	$P_k(T)$	$P_k(e)$	$[P_k(T)]^2$	j	r_1	r_2	Proved
2.1				-1	0	0	No
2.2				0	0.5	1	No
2.3	$P_0(T)$	$P_0(e)$	$[P_0(T)]^2$	1	0	0	No
2.4				∞	$-\infty$	$-\infty$	No
2.5				-1	1	2	Y/N
2.6				0	1.5	2	No
2.7	$P_1(T)$	$P_1(e)$	$[P_1(T)]^2$	1	1	1	No
2.8				∞	$-\infty$	$-\infty$	No
2.9				-1	2	3	Y/N
2.10				0	2.5	3	No
2.11	$P_2(T)$	$P_2(e)$	$[P_2(T)]^2$	1	2	2	No
2.12				∞	$-\infty$	$-\infty$	No

3. The WG elements with $\ell = s$ on rectangular mesh

Next we will study convergence rate for the WG element $(P_\ell(T), P_s(e), G_m(T))$ with $\ell = s$ on rectangular meshes. The rectangular meshes used in the computation are illustrated in Figure 1.

Table 1 demonstrates the convergence rates for $(P_k(T), P_k(e), [P_{k-1}(T)]^2)$ with a stabilizer of different j defined in (10) on rectangular mesh.

Table 2 demonstrates the convergence rates for $(P_k(T), P_k(e), [P_k(T)]^2)$ with a stabilizer of different j on rectangular mesh.

Remark 2. *Theorem 4.9 in* [16] *guarantees the optimal convergence rate of the WG element 2.5 in the* $|||\cdot|||$ *norm. However the optimal convergence rate in the* L^2 *norm is not proved in* [16]. *Therefore, we still mark proved* $= Y/N$ *in the case 2.5.*

TABLE 3. Element $(P_k(T), P_k(e), [P_{k+1}(T)]^2)$ on rectangular mesh, $|||\cdot||| = O(h^{r_1})$ and $\|\cdot\| = O(h^{r_2})$.

element	$P_k(T)$	$P_k(e)$	$[P_{k+1}(T)]^2$	j	r_1	r_2	Proved
3.1				-1	0	0	No
3.2				0	1	1	No
3.3	$P_0(T)$	$P_0(e)$	$[P_1(T)]^2$	1	2	2	No
3.4				∞	2	2	No
3.5				-1	1	2	Y/N
3.6				0	2	3	No
3.7	$P_1(T)$	$P_1(e)$	$[P_2(T)]^2$	1	3	4	No
3.8				∞	3	4	Yes
3.9				-1	2	3	Y/N
3.10				0	3	4	No
3.11	$P_2(T)$	$P_2(e)$	$[P_3(T)]^2$	1	4	5	No
3.12				∞	4	5	Yes

TABLE 4. Element $(P_k(T), P_k(e), [P_{k+2}(T)]^2)$ on rectangular mesh, $|||\cdot||| = O(h^{r_1})$ and $\|\cdot\| = O(h^{r_2})$.

element	$P_k(T)$	$P_k(e)$	$[P_{k+2}(T)]^2$	j	r_1	r_2	Proved
4.1				-1	0	0	No
4.2				0	0	0	No
4.3	$P_0(T)$	$P_0(e)$	$[P_2(T)]^2$	1	0	0	No
4.4				∞	0	0	No
4.5				-1	1	2	Y/N
4.6				0	1	2	No
4.7	$P_1(T)$	$P_1(e)$	$[P_3(T)]^2$	1	1	2	No
4.8				∞	1	2	Yes
4.9				-1	2	3	Y/N
4.10				0	2	3	No
4.11	$P_2(T)$	$P_2(e)$	$[P_4(T)]^2$	1	2	3	No
4.12				∞	2	3	Yes

Table 3 demonstrates the convergence rates for $(P_k(T), P_k(e), [P_{k+1}(T)]^2)$ with a stabilizer of different j on rectangular mesh.

Table 4 demonstrates the convergence rates for $(P_k(T), P_k(e), [P_{k+2}(T)]^2)$ with a stabilizer of different j on rectangular mesh.

Remark 3. *For the $P_k(T) - P_k(e)$ element, Tables 1-4 demonstrate that the performance of the WG solutions are getting better when the degree of the polynomials for weak gradient is increasing from $k-1$ to $k+1$. Specially the WG element $(P_k(T), P_k(e), [P_{k+1}(T)]^2)$ shows order two supercloseness in Table 3. However, for the element $(P_k(T), P_k(e), [P_{k+2}(T)]^2$, the numerical tests in Table 4 show the convergence rate of the WG solution decreasing. Remember that increasing m in $[P_m(T)]^2$ for weak gradient does not introduce additional degrees of freedom for the resulting linear systems.*

Table 5 demonstrates the convergence rates for $(P_k(T), P_k(e), RT_k(T))$ with a stabilizer of different j on rectangular mesh.

4. The WG elements for $\ell = s$ on triangular mesh

The triangular meshes used in the computation are displayed in Figure 2.

Table 6 demonstrates the convergence rates for $(P_k(T), P_k(e), [P_{k-1}(T)]^2)$ with a stabilizer of different j on triangular mesh.

Table 7 demonstrates the convergence rates for $(P_k(T), P_k(e), [P_k(T)]^2)$ with a stabilizer of different j on triangular mesh.

Table 8 demonstrates the convergence rates for $(P_k(T), P_k(e), [P_{k+1}(T)]^2)$ with a stabilizer of different j on triangular mesh.

TABLE 5. Element $(P_k(T), P_k(e), RT_k(T))$ on rectangular mesh, $|||\cdot||| = O(h^{r_1})$ and $\|\cdot\| = O(h^{r_2})$.

element	$P_k(T)$	$P_k(e)$	$RT_k(T)$	j	r_1	r_2	Proved
5.1				-1	0	0	No
5.2				0	1	1	No
5.3	$P_0(T)$	$P_0(e)$	$RT_0(T)$	1	2	2	No
5.4				∞	2	2	No
5.5				-1	1	2	No
5.6				0	1.5	2	No
5.7	$P_1(T)$	$P_1(e)$	$RT_1(T)$	1	1	1	No
5.8				∞	1	1	No
5.9				-1	2	3	No
5.10				0	2.5	3	No
5.11	$P_2(T)$	$P_2(e)$	$RT_2(T)$	1	2	2	No
5.12				∞	2	2	No

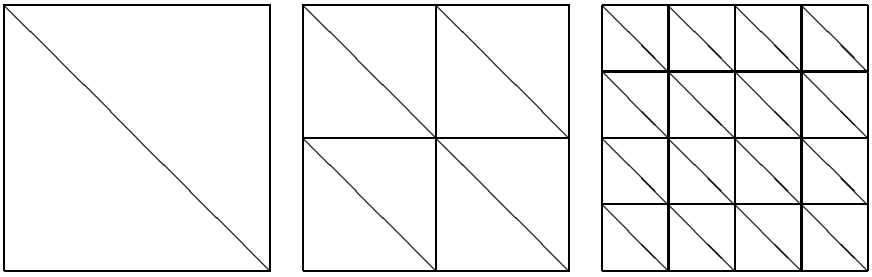

FIGURE 2. The first three level triangular meshes.

TABLE 6. Element $(P_k(T), P_k(e), [P_{k-1}(T)]^2)$ on triangular mesh, $|||\cdot||| = O(h^{r_1})$ and $\|\cdot\| = O(h^{r_2})$.

element	$P_k(T)$	$P_k(e)$	$[P_{k-1}(T)]^2$	j	r_1	r_2	Proved
6.1				-1	1	2	Yes
6.2				0	0.5	1	No
6.3	$P_1(T)$	$P_1(e)$	$[P_0(T)]^2$	1	0	0	No
6.4				∞	$-\infty$	$-\infty$	No
6.5				-1	2	3	Yes
6.6				0	1.5	2	No
6.7	$P_2(T)$	$P_2(e)$	$[P_1(T)]^2$	1	1	1	No
6.8				∞	$-\infty$	$-\infty$	No
6.9				-1	3	4	Yes
6.10				0	2.5	3	No
6.11	$P_3(T)$	$P_3(e)$	$[P_2(T)]^2$	1	2	2	No
6.12				∞	$-\infty$	$-\infty$	No

TABLE 7. Element $(P_k(T), P_k(e), [P_k(T)]^2)$ on triangular mesh, $|||\cdot||| = O(h^{r_1})$ and $\|\cdot\| = O(h^{r_2})$.

element	$P_k(T)$	$P_k(e)$	$[P_k(T)]^2$	j	r_1	r_2	Proved
7.1				-1	0	0	No
7.2				0	0.5	1	No
7.3	$P_0(T)$	$P_0(e)$	$[P_0(T)]^2$	1	0	0	No
7.4				∞	$-\infty$	$-\infty$	No
7.5				-1	1	2	Y/N
7.6				0	1.5	2	No
7.7	$P_1(T)$	$P_1(e)$	$[P_1(T)]^2$	1	1	1	No
7.8				∞	$-\infty$	$-\infty$	No
7.9				-1	2	3	Y/N
7.10				0	2.5	3	No
7.11	$P_2(T)$	$P_2(e)$	$[P_2(T)]^2$	1	2	2	No
7.12				∞	$-\infty$	$-\infty$	No

TABLE 8. Element $(P_k(T), P_k(e), [P_{k+1}(T)]^2)$ on triangular mesh, $|||\cdot||| = O(h^{r_1})$ and $\|\cdot\| = O(h^{r_2})$.

element	$P_k(T)$	$P_k(e)$	$[P_{k+1}(T)]^2$	j	r_1	r_2	Proved
8.1				-1	0	0	No
8.2				0	0	0	No
8.3	$P_0(T)$	$P_0(e)$	$[P_1(T)]^2$	1	0	0	No
8.4				∞	0	0	No
8.5				-1	1	2	Y/N
8.6				0	1	2	No
8.7	$P_1(T)$	$P_1(e)$	$[P_2(T)]^2$	1	1	2	No
8.8				∞	1	2	Yes
8.9				-1	2	3	Y/N
8.10				0	2	3	No
8.11	$P_2(T)$	$P_2(e)$	$[P_3(T)]^2$	1	2	3	No
8.12				∞	2	3	Yes

TABLE 9. Element $(P_k(T), P_k(e), RT_k(T))$ on triangular mesh, $|||\cdot||| = O(h^{r_1})$ and $\|\cdot\| = O(h^{r_2})$.

element	$P_k(T)$	$P_k(e)$	$RT_k(T)$	j	r_1	r_2	Proved
9.1				-1	0	0	No
9.2				0	1	1	No
9.3	$P_0(T)$	$P_0(e)$	$RT_0(T)$	1	1	2	No
9.4				∞	1	2	Yes
9.5				-1	1	2	No
9.6				0	2	3	No
9.7	$P_1(T)$	$P_1(e)$	$RT_1(T)$	1	2	3	No
9.8				∞	2	3	Yes
9.9				-1	2	3	No
9.10				0	3	4	No
9.11	$P_2(T)$	$P_2(e)$	$RT_2(T)$	1	3	4	No
9.12				∞	3	4	Yes

TABLE 10. Element $(P_k(T), P_{k+1}(e), [P_{k-1}(T)]^2)$ on rectangular mesh, $|||\cdot||| = O(h^{r_1})$ and $\|\cdot\| = O(h^{r_2})$.

element	$P_k(T)$	$P_{k+1}(e)$	$[P_{k-1}(T)]^d$	j	r_1	r_2	Proved
10.1				-1	1	2	Y/N
10.2				0	0.5	1	No
10.3	$P_1(T)$	$P_2(e)$	$[P_0(T)]^2$	1	0	0	No
10.4				∞	$-\infty$	$-\infty$	No
10.5				-1	2	3	Y/N
10.6				0	1.5	2	No
10.7	$P_2(T)$	$P_3(e)$	$[P_1(T)]^2$	1	1	1	No
10.8				∞	$-\infty$	$-\infty$	No
10.9				-1	3	4	Y/N
10.10				0	2.5	3	No
10.11	$P_3(T)$	$P_4(e)$	$[P_2(T)]^2$	1	2	2	No
10.12				∞	$-\infty$	$-\infty$	No

Remark 4. *The WG element $(P_k(T), P_k(e), [P_{k+1}(T)]^2)$ performs much better on rectangular meshes than triangular meshes.*

Table 9 demonstrates the convergence rates for $(P_k(T), P_k(e), RT_k(T))$ with a stabilizer of different j on triangular mesh.

5. The WG elements with $\ell < s$ on rectangular mesh

The following table demonstrates the convergence rates for $(P_k(T), P_{k+1}(e), [P_{k-1}(T)]^2)$ with a stabilizer of different j on rectangular mesh.

The following table demonstrates the convergence rates for $(P_k(T), P_{k+1}(e), [P_k(T)]^2)$ with a stabilizer of different j on rectangular mesh.

Table 12 demonstrates the convergence rates for $(P_k(T), P_{k+1}(e), [P_{k+1}(T)]^2)$ with a stabilizer of different j on rectangular mesh.

TABLE 11. Element $(P_k(T), P_{k+1}(e), [P_k(T)]^2)$ on rectangular mesh, $|||\cdot||| = O(h^{r_1})$ and $\|\cdot\| = O(h^{r_2})$.

element	$P_k(T)$	$P_{k+1}(e)$	$[P_k(T)]^2$	j	r_1	r_2	Proved
11.1				-1	0	0	No
11.2				0	0.5	1	No
11.3	$P_0(T)$	$P_1(e)$	$[P_0(T)]^2$	1	0	0	No
11.4				∞	$-\infty$	$-\infty$	No
11.5				-1	1	2	Y/N
11.6				0	1.5	2	No
11.7	$P_1(T)$	$P_2(e)$	$[P_1(T)]^2$	1	1	1	No
11.8				∞	$-\infty$	$-\infty$	No
11.9				-1	2	3	Y/N
11.10				0	2.5	3	No
11.11	$P_2(T)$	$P_3(e)$	$[P_2(T)]^2$	1	2	2	No
11.12				∞	$-\infty$	$-\infty$	No

TABLE 12. Element $(P_k(T), P_{k+1}(e), [P_{k+1}(T)]^2)$ on rectangular mesh, $|||\cdot||| = O(h^{r_1})$ and $\|\cdot\| = O(h^{r_2})$.

element	$P_k(T)$	$P_{k+1}(e)$	$[P_{k+1}(T)]^2$	j	r_1	r_2	Proved
12.1				-1	0	0	No
12.2				0	0.5	1	No
12.3	$P_0(T)$	$P_1(e)$	$[P_1(T)]^2$	1	1	2	No
12.4				∞	1	2	No
12.5				-1	1	2	Y/N
12.6				0	1.5	3	No
12.7	$P_1(T)$	$P_2(e)$	$[P_2(T)]^2$	1	2	4	No
12.8				∞	2	4	No
12.9				-1	2	3	Y/N
12.10				0	2.5	4	No
12.11	$P_2(T)$	$P_3(e)$	$[P_3(T)]^2$	1	3	5	No
12.12				∞	3	5	No

TABLE 13. Element $(P_k(T), P_{k+1}(e), [P_{k+2}(T)]^2)$ on rectangular mesh, $|||\cdot||| = O(h^{r_1})$ and $\|\cdot\| = O(h^{r_2})$.

element	$P_k(T)$	$P_{k+1}(e)$	$[P_{k+2}(T)]^2$	j	r_1	r_2	Proved
13.1				-1	0	0	No
13.2				0	0	0	No
13.3	$P_0(T)$	$P_1(e)$	$[P_2(T)]^2$	1	0	0	No
13.4				∞	0	0	No
13.5				-1	1	2	Y/N
13.6				0	1	2	No
13.7	$P_1(T)$	$P_2(e)$	$[P_3(T)]^2$	1	1	2	No
13.8				∞	1	2	No
13.9				-1	2	3	Y/N
13.10				0	2	3	No
13.11	$P_2(T)$	$P_3(e)$	$[P_4(T)]^2$	1	2	3	No
13.12				∞	2	3	No

Table 13 demonstrates the convergence rates for $(P_k(T), P_{k+1}(e), [P_{k+2}(T)]^2)$ with a stabilizer of different j on rectangular mesh.

Remark 5. *The WG element $(P_k(T), P_{k+1}(e), [P_{k+1}(T)]^2)$ performs better than WG element $(P_k(T), P_{k+1}(e), [P_{k+2}(T)]^2)$ although the later element uses higher degree polynomials for weak gradient.*

Table 14 demonstrates the convergence rates for $(P_k(T), P_{k+1}(e), RT_k(T))$ with a stabilizer of different j on rectangular mesh.

Table 15 demonstrates the convergence rates for $(P_k(T), P_{k+1}(e), RT_{k+1}(T))$ with a stabilizer of different j on rectangular mesh.

TABLE 14. Element $(P_k(T), P_{k+1}(e), RT_k(T))$ on rectangular mesh, $|||\cdot||| = O(h^{r_1})$ and $\|\cdot\| = O(h^{r_2})$.

element	$P_k(T)$	$P_{k+1}(e)$	$RT_k(T)$	j	r_1	r_2	Proved
14.1				-1	0	0	No
14.2				0	0.5	1	No
14.3	$P_0(T)$	$P_1(e)$	$RT_0(T)$	1	1	2	No
14.4				∞	2	2	No
14.5				-1	1	2	No
14.6				0	1.5	2	No
14.7	$P_1(T)$	$P_2(e)$	$RT_1(T)$	1	1	1	No
14.8				∞	$-\infty$	$-\infty$	No
14.9				-1	2	3	No
14.10				0	2.5	3	No
14.11	$P_2(T)$	$P_3(e)$	$RT_2(T)$	1	2	2	No
14.12				∞	$-\infty$	$-\infty$	No

TABLE 15. Element $(P_k(T), P_{k+1}(e), RT_{k+1}(T))$ on rectangular mesh, $|||\cdot||| = O(h^{r_1})$ and $\|\cdot\| = O(h^{r_2})$.

element	$P_k(T)$	$P_{k+1}(e)$	$RT_{k+1}(T)$	j	r_1	r_2	Proved
15.1				-1	0	0	No
15.2				0	0	1	No
15.3	$P_0(T)$	$P_1(e)$	$RT_1(T)$	1	0	2	No
15.4				∞	0	2	No
15.5				-1	1	2	No
15.6				0	1	2	No
15.7	$P_1(T)$	$P_2(e)$	$RT_2(T)$	1	1	2	No
15.8				∞	1	2	No
15.9				-1	2	4	No
15.10				0	2	4	No
15.11	$P_2(T)$	$P_3(e)$	$RT_3(T)$	1	2	4	No
15.12				∞	2	4	No

TABLE 16. Element $(P_k(T), P_{k+1}(e), [P_{k-1}(T)]^2)$ on triangular mesh, $|||\cdot||| = O(h^{r_1})$ and $\|\cdot\| = O(h^{r_2})$.

element	$P_k(T)$	$P_{k+1}(e)$	$[P_{k-1}(T)]^2$	j	r_1	r_2	Proved
16.1				-1	1	2	Y/N
16.2				0	0.5	1	No
16.3	$P_1(T)$	$P_2(e)$	$[P_0(T)]^2$	1	0	0	No
16.4				∞	$-\infty$	$-\infty$	No
16.5				-1	2	3	Y/N
16.6				0	1.5	2	No
16.7	$P_2(T)$	$P_3(e)$	$[P_1(T)]^2$	1	1	1	No
16.8				∞	$-\infty$	$-\infty$	No
16.9				-1	3	4	Y/N
16.10				0	2.5	3	No
16.11	$P_3(T)$	$P_4(e)$	$[P_2(T)]^2$	1	2	2	No
16.12				∞	$-\infty$	$-\infty$	No

6. The WG elements for $\ell < s$ on triangular mesh

Table 16 demonstrates the convergence rates for $(P_k(T), P_{k+1}(e), [P_{k-1}(T)]^2)$ with a stabilizer of different j on triangular mesh.

Table 17 demonstrates the convergence rates for $(P_k(T), P_{k+1}(e), [P_k(T)]^2)$ with a stabilizer of different j on triangular mesh.

Table 18 demonstrates the convergence rates for $(P_k(T), P_{k+1}(e), [P_{k+1}(T)]^2)$ with a stabilizer of different j on triangular mesh.

Remark 6. *The WG element $(P_k(T), P_{k+1}(e), [P_{k+1}(T)]^2)$ has order two supercloseness on triangular mesh.*

Table 19 demonstrates the convergence rates for $(P_k(T), P_{k+1}(e), [P_{k+2}(T)]^2)$ with a stabilizer of different j on triangular mesh.

TABLE 17. Element $(P_k(T), P_{k+1}(e), [P_k(T)]^2)$ on triangular mesh, $|||\cdot||| = O(h^{r_1})$ and $\|\cdot\| = O(h^{r_2})$.

element	$P_k(T)$	$P_{k+1}(e)$	$[P_k(T)]^2$	j	r_1	r_2	Proved
17.1				-1	0	0	No
17.2				0	0.5	1	No
17.3	$P_0(T)$	$P_1(e)$	$[P_0(T)]^2$	1	0	0	No
17.4				∞	$-\infty$	$-\infty$	No
17.5				-1	1	2	Y/N
17.6				0	1.5	2	No
17.7	$P_1(T)$	$P_2(e)$	$[P_1(T)]^2$	1	1	1	No
17.8				∞	$-\infty$	$-\infty$	No
17.9				-1	2	3	Y/N
17.10				0	2.5	3	No
17.11	$P_2(T)$	$P_3(e)$	$[P_2(T)]^2$	1	2	2	No
17.12				∞	$-\infty$	$-\infty$	No

TABLE 18. Element $(P_k(T), P_{k+1}(e), [P_{k+1}(T)]^2)$ on triangular mesh, $|||\cdot||| = O(h^{r_1})$ and $\|\cdot\| = O(h^{r_2})$.

element	$P_k(T)$	$P_{k+1}(e)$	$[P_{k+1}(T)]^2$	j	r_1	r_2	Proved
18.1				-1	0	0	No
18.2				0	1	1	No
18.3	$P_0(T)$	$P_1(e)$	$[P_1(T)]^2$	1	2	2	No
18.4				∞	2	2	Yes
18.5				-1	1	2	Y/N
18.6				0	2	3	No
18.7	$P_1(T)$	$P_2(e)$	$[P_2(T)]^2$	1	3	4	No
18.8				∞	3	4	Yes
18.9				-1	2	3	Y/N
18.10				0	3	4	No
18.11	$P_2(T)$	$P_3(e)$	$[P_3(T)]^2$	1	4	5	No
18.12				∞	4	5	Yes

TABLE 19. Element $(P_k(T), P_{k+1}(e), [P_{k+2}(T)]^2)$ on triangular mesh, $|||\cdot||| = O(h^{r_1})$ and $\|\cdot\| = O(h^{r_2})$.

element	$P_k(T)$	$P_{k+1}(e)$	$[P_{k+2}(T)]^2$	j	r_1	r_2	Proved
19.1				-1	0	0	No
19.2				0	0	0	No
19.3	$P_0(T)$	$P_1(e)$	$[P_2(T)]^2$	1	0	0	No
19.4				∞	0	0	No
19.5				-1	1	2	Y/N
19.6				0	1	2	No
19.7	$P_1(T)$	$P_2(e)$	$[P_3(T)]^2$	1	1	2	No
19.8				∞	1	2	No
19.9				-1	2	3	Y/N
19.10				0	2	3	No
19.11	$P_2(T)$	$P_3(e)$	$[P_4(T)]^2$	1	2	3	No
19.12				∞	2	3	No

Table 20 demonstrates the convergence rates for $(P_k(T), P_{k+1}(e), RT_k(T))$ with a stabilizer of different j on triangular mesh.

Table 21 demonstrates the convergence rates for $(P_k(T), P_{k+1}(e), RT_{k+1}(T))$ with a stabilizer of different j on triangular mesh.

7. The WG elements for $\ell > s$ on rectangular mesh

Table 22 demonstrates the convergence rates for $(P_k(T), P_{k-1}(e), [P_{k-1}(T)]^2)$ with a stabilizer of different j on rectangular mesh.

Table 23 demonstrates the convergence rates for $(P_k(T), P_{k-1}(e), [P_k(T)]^2)$ with a stabilizer of different j on rectangular mesh.

Remark 7. *The WG element 23.1 achieves optimal convergence rates on triangular mesh while Theorem 4.9 in* [16] *predict only suboptimal convergence rate.*

TABLE 20. Element $(P_k(T), P_{k+1}(e), RT_k(T))$ on triangular mesh, $|||\cdot||| = O(h^{r_1})$ and $\|\cdot\| = O(h^{r_2})$.

element	$P_k(T)$	$P_{k+1}(e)$	$RT_k(T)$	j	r_1	r_2	Proved
20.1				-1	0	0	No
20.2				0	0.5	1	No
20.3	$P_0(T)$	$P_1(e)$	$RT_0(T)$	1	1	2	No
20.4				∞	1	2	No
20.5				-1	1	2	No
20.6				0	1.5	3	No
20.7	$P_1(T)$	$P_2(e)$	$RT_1(T)$	1	2	3	No
20.8				∞	$-\infty$	$-\infty$	No
20.9				-1	2	3	No
20.10				0	2.5	4	No
20.11	$P_2(T)$	$P_3(e)$	$RT_2(T)$	1	3	4	No
20.12				∞	$-\infty$	$-\infty$	No

TABLE 21. Element $(P_k(T), P_{k+1}(e), RT_{k+1}(T))$ on triangular mesh, $|||\cdot||| = O(h^{r_1})$ and $\|\cdot\| = O(h^{r_2})$.

element	$P_k(T)$	$P_{k+1}(e)$	$RT_{k+1}(T)$	j	r_1	r_2	Proved
21.1				-1	0	0	No
21.2				0	0	0	No
21.3	$P_0(T)$	$P_1(e)$	$RT_1(T)$	1	0	0	No
21.4				∞	0	0	No
21.5				-1	1	2	No
21.6				0	1	2	No
21.7	$P_1(T)$	$P_2(e)$	$RT_2(T)$	1	1	2	No
21.8				∞	1	2	No
21.9				-1	2	3	No
21.10				0	2	3	No
21.11	$P_2(T)$	$P_3(e)$	$RT_3(T)$	1	2	3	No
21.12				∞	2	3	No

TABLE 22. Element $(P_k(T), P_{k-1}(e), [P_{k-1}(T)]^2)$ on rectangular mesh, $|||\cdot||| = O(h^{r_1})$ and $\|\cdot\| = O(h^{r_2})$.

element	$P_k(T)$	$P_{k-1}(e)$	$[P_{k-1}(T)]^d$	j	r_1	r_2	Proved
22.1				-1	1	2	Yes
22.2				0	0.5	1	No
22.3	$P_1(T)$	$P_0(e)$	$[P_0(T)]^2$	1	0	0	No
22.4				∞	$-\infty$	$-\infty$	No
22.5				-1	2	3	Yes
22.6				0	1.5	2	No
22.7	$P_2(T)$	$P_1(e)$	$[P_1(T)]^2$	1	1	1	No
22.8				∞	$-\infty$	$-\infty$	No
22.9				-1	3	4	Yes
22.10				0	2.5	3	No
22.11	$P_3(T)$	$P_2(e)$	$[P_2(T)]^2$	1	2	2	No
22.12				∞	$-\infty$	$-\infty$	No

TABLE 23. Element $(P_k(T), P_{k-1}(e), [P_k(T)]^2)$ on rectangular mesh, $|||\cdot||| = O(h^{r_1})$ and $\|\cdot\| = O(h^{r_2})$.

element	$P_k(T)$	$P_{k-1}(e)$	$[P_k(T)]^d$	j	r_1	r_2	Proved
23.1				-1	1	2	No
23.2				0	1.5	2	No
23.3	$P_1(T)$	$P_0(e)$	$[P_1(T)]^2$	1	1	1	No
23.4				∞	$-\infty$	$-\infty$	No
23.5				-1	2	3	No
23.6				0	2.5	3	No
23.7	$P_2(T)$	$P_1(e)$	$[P_2(T)]^2$	1	2	2	No
23.8				∞	$-\infty$	$-\infty$	No
23.9				-1	3	4	No
23.10				0	3.5	4	No
23.11	$P_3(T)$	$P_2(e)$	$[P_3(T)]^2$	1	3	3	No
23.12				∞	$-\infty$	$-\infty$	No

TABLE 24. Element $(P_k(T), P_{k-1}(e), [P_{k+1}(T)]^2)$ on rectangular mesh, $|||\cdot||| = O(h^{r_1})$ and $\|\cdot\| = O(h^{r_2})$.

element	$P_k(T)$	$P_{k-1}(e)$	$[P_{k+1}(T)]^d$	j	r_1	r_2	Proved
24.1				-1	0	0	No
24.2				0	0	0	No
24.3	$P_1(T)$	$P_0(e)$	$[P_2(T)]^2$	1	0	0	No
24.4				∞	0	0	No
24.5				-1	1	2	Y/N
24.6				0	1	2	No
24.7	$P_2(T)$	$P_1(e)$	$[P_3(T)]^2$	1	1	2	No
24.8				∞	1	2	No
24.9				-1	2	3	Y/N
24.10				0	2	3	No
24.11	$P_3(T)$	$P_2(e)$	$[P_4(T)]^2$	1	2	3	No
24.12				∞	2	3	No

TABLE 25. Element $(P_k(T), P_{k-1}(e), RT_{k-1}(T))$ on rectangular mesh, $|||\cdot||| = O(h^{r_1})$ and $\|\cdot\| = O(h^{r_2})$.

element	$P_k(T)$	$P_{k-1}(e)$	$RT_{k-1}(T)$	j	r_1	r_2	Proved
25.1				-1	1	2	No
25.2				0	1.5	2	No
25.3	$P_1(T)$	$P_0(e)$	$RT_0(T)$	1	1	1	No
25.4				∞	$-\infty$	$-\infty$	No
25.5				-1	2	3	No
25.6				0	1.5	2	No
25.7	$P_2(T)$	$P_1(e)$	$RT_1(T)$	1	1	1	No
25.8				∞	$-\infty$	$-\infty$	No
25.9				-1	3	4	No
25.10				0	2.5	3	No
25.11	$P_3(T)$	$P_2(e)$	$RT_2(T)$	1	2	2	No
25.12				∞	$-\infty$	$-\infty$	No

TABLE 26. Element $(P_k(T), P_{k-1}(e), RT_k(T))$ on rectangular mesh, $|||\cdot||| = O(h^{r_1})$ and $\|\cdot\| = O(h^{r_2})$.

element	$P_k(T)$	$P_{k-1}(e)$	$RT_k(T)$	j	r_1	r_2	Proved
26.1				-1	0	0	No
26.2				0	0	1	No
26.3	$P_1(T)$	$P_0(e)$	$RT_1(T)$	1	0	1	No
26.4				∞	0	1	No
26.5				-1	1	2	No
26.6				0	1	2	No
26.7	$P_2(T)$	$P_1(e)$	$RT_2(T)$	1	1	2	No
26.8				∞	1	2	No
26.9				-1	2	3	No
26.10				0	2	3	No
26.11	$P_3(T)$	$P_2(e)$	$RT_3(T)$	1	2	3	No
26.12				∞	2	3	No

Table 24 demonstrates the convergence rates for $(P_k(T), P_{k-1}(e), [P_{k+1}(T)]^2)$ with a stabilizer of different j on rectangular mesh.

Remark 8. *The numerical results in Table 24 show that the WG element* $(P_k(T), P_{k-1}(e), [P_{k+1}(T)]^2)$ *has suboptimal convergence rates on rectangular mesh. A new stabilizer free WG method is proposed in* [22] *for the element* $(P_k(T), P_{k-1}(e), [P_{k+1}(T)]^2)$ *with optimal convergence rate, on general polygonal meshes.*

Table 25 demonstrates the convergence rates for $(P_k(T), P_{k-1}(e), RT_{k-1}(T))$ with a stabilizer of different j on rectangular mesh.

Table 26 demonstrates the convergence rates for $(P_k(T), P_{k-1}(e), RT_k(T))$ with a stabilizer of different j on rectangular mesh.

TABLE 27. Element $(P_k(T), P_{k-1}(e), [P_{k-1}(T))$ on triangular mesh, $|||\cdot||| = O(h^{r_1})$ and $\|\cdot\| = O(h^{r_2})$.

element	$P_k(T)$	$P_{k-1}(e)$	$[P_{k-1}(T)]^2$	j	r_1	r_2	Proved
27.1				-1	1	2	Yes
27.2				0	0.5	1	No
27.3	$P_1(T)$	$P_0(e)$	$[P_0(T)]^2$	1	0	0	No
27.4				∞	$-\infty$	$-\infty$	No
27.5				-1	2	3	Yes
27.6				0	1.5	2	No
27.7	$P_2(T)$	$P_1(e)$	$[P_1(T)]^2$	1	1	1	No
27.8				∞	$-\infty$	$-\infty$	No
27.9				-1	3	4	Yes
27.10				0	2.5	3	No
27.11	$P_3(T)$	$P_2(e)$	$[P_2(T)]^2$	1	2	2	No
27.12				∞	$-\infty$	$-\infty$	No

TABLE 28. Element $((P_k(T), P_{k-1}(e), [P_k(T)]^2))$ on triangular mesh, $|||\cdot||| = O(h^{r_1})$ and $\|\cdot\| = O(h^{r_2})$.

element	$P_k(T)$	$P_{k-1}(e)$	$[P_k(T)]^2$	j	r_1	r_2	Proved
28.1				-1	0	0	Y/N
28.2				0	0	0	No
28.3	$P_1(T)$	$P_0(e)$	$[P_1(T)]^2$	1	0	0	No
28.4				∞	$-\infty$	$-\infty$	No
28.5				-1	1	2	Y/N
28.6				0	1	2	No
28.7	$P_2(T)$	$P_1(e)$	$[P_2(T)]^2$	1	1	2	No
28.8				∞	$-\infty$	$-\infty$	No
28.9				-1	2	3	Y/N
28.10				0	2	3	No
28.11	$P_3(T)$	$P_2(e)$	$[P_3(T)]^2$	1	2	3	No
28.12				∞	$-\infty$	$-\infty$	No

TABLE 29. Element $((P_k(T), P_{k-1}(e), [P_{k+1}(T)]^2))$ on triangular mesh, $|||\cdot||| = O(h^{r_1})$ and $\|\cdot\| = O(h^{r_2})$.

element	$P_k(T)$	$P_{k-1}(e)$	$[P_{k+1}(T)]^2$	j	r_1	r_2	Proved
29.1				-1	0	0	Y/N
29.2				0	0	0	No
29.3	$P_1(T)$	$P_0(e)$	$[P_2(T)]^2$	1	0	0	No
29.4				∞	0	0	No
29.5				-1	1	2	Y/N
29.6				0	1	2	No
29.7	$P_2(T)$	$P_1(e)$	$[P_3(T)]^2$	1	1	2	No
29.8				∞	1	2	No
29.9				-1	2	3	Y/N
29.10				0	2	3	No
29.11	$P_3(T)$	$P_2(e)$	$[P_4(T)]^2$	1	2	3	No
29.12				∞	2	3	No

8. The WG elements for $\ell > s$ on triangular mesh

Table 27 demonstrates the convergence rates for $(P_k(T), P_{k-1}(e), [P_{k-1}(T)]^2)$ with a stabilizer of different j on triangular mesh.

Table 28 demonstrates the convergence rates for $(P_k(T), P_{k-1}(e), [P_k(T)]^2)$ with a stabilizer of different j on triangular mesh.

Remark 9. *The WG element $(P_k(T), P_{k-1}(e), [P_k(T)]^2)$ performs better on rectangular mesh than on triangular mesh.*

Table 29 demonstrates the convergence rates for $(P_k(T), P_{k-1}(e), [P_{k+1}(T)]^2)$ with a stabilizer of different j on triangular mesh.

Table 30 demonstrates the convergence rates for $(P_k(T), P_{k-1}(e), RT_{k-1}(T))$ with a stabilizer of different j on triangular mesh.

TABLE 30. Element $(P_k(T), P_{k-1}(e), RT_{k-1}(T))$ on triangular mesh, $|||\cdot||| = O(h^{r_1})$ and $\|\cdot\| = O(h^{r_2})$.

element	$P_k(T)$	$P_{k-1}(e)$	$RT_{k-1}(T)$	j	r_1	r_2	Proved
30.1				-1	1	2	No
30.2				0	1	2	No
30.3	$P_1(T)$	$P_0(e)$	$RT_0(T)$	1	1	1	No
30.4				∞	$-\infty$	$-\infty$	No
30.5				-1	2	3	No
30.6				0	2	3	No
30.7	$P_2(T)$	$P_1(e)$	$RT_1(T)$	1	2	2	No
30.8				∞	$-\infty$	$-\infty$	No
30.9				-1	3	4	No
30.10				0	3	4	No
30.11	$P_3(T)$	$P_2(e)$	$RT_2(T)$	1	3	3	No
30.12				∞	$-\infty$	$-\infty$	No

TABLE 31. Element $(P_k(T), P_{k-1}(e), RT_k(T))$ on triangular mesh, $|||\cdot||| = O(h^{r_1})$ and $\|\cdot\| = O(h^{r_2})$.

element	$P_k(T)$	$P_{k-1}(e)$	$RT_k(T)$	j	r_1	r_2	Proved
31.1				-1	0	0	No
31.2				0	0	0	No
31.3	$P_1(T)$	$P_0(e)$	$RT_1(T)$	1	0	0	No
31.4				∞	0	0	No
31.5				-1	1	2	No
31.6				0	1	2	No
31.7	$P_2(T)$	$P_1(e)$	$RT_2(T)$	1	1	2	No
31.8				∞	1	2	No
31.9				-1	2	3	No
31.10				0	2	3	No
31.11	$P_3(T)$	$P_2(e)$	$RT_3(T)$	1	2	3	No
31.12				∞	2	3	No

Table 31 demonstrates the convergence rates for $(P_k(T), P_{k-1}(e), RT_k(T))$ with a stabilizer of different j on triangular mesh.

Acknowledgments

The research of Junping Wang was supported by the NSF IR/D program, while working at National Science Foundation. However, any opinion, finding, and conclusions or recommendations expressed in this material are those of the author and do not necessarily reflect the views of the National Science Foundation. The research of Xiu Ye was supported in part by National Science Foundation Grant DMS-1620016.

References

[1] A. Al-Taweel and X. Wang, A note on the optimal degree of the weak gradient of the stabilizer free weak Galerkin finite element method, Appl. Numer. Math. 150 (2020), 444-451.
[2] A. Al-Taweel, X. Wang, X. Ye and S. Zhang, A stabilizer free weak Galerkin element method with supercloseness of order two, priprint.
[3] F. Brezzi and M. Fortin, Mixed and Hybrid Finite Elements, Springer-Verlag, New York, 1991.
[4] M. Cui and S. Zhang, On the uniform convergence of the weak Galerkin finite element method for a singularly-perturbed biharmonic equation, J. Sci. Comput. 82 (2020), no. 1, Paper No. 5, 15 pp.
[5] X. Hu, L. Mu and X. Ye, A weak Galerkin finite element method for the Navier-Stokes equations on polytopal meshes, J. Comput. Appl. Math. 362 (2019), 614-625.
[6] R. Lin, X. Ye, S. Zhang and P. Zhu, A weak Galerkin finite element method for singularly perturbed convection-diffusion-reaction problems, SIAM J. Numer. Anal. 56 (2018), 1482-1497.
[7] G. Lin, J. Liu, L.Mu and X. Ye, weak Galerkin finite element methods for Darcy flow: Anisotropy and heterogeneity, J. Comput. Phy. 276 (2014), 422-437.

[8] L. Mu, J. Wang and X. Ye, weak Galerkin finite element method for the Helmholtz equation with large wave number on polytopal meshes, IMA J. Numer. Anal. 35 (2015), 1228-1255.
[9] L. Mu, J. Wang, and X. Ye, A stable numerical algorithm for the Brinkman equations by weak Galerkin finite element methods, J. Comput. Phys. 273 (2014), 327-342.
[10] L. Mu, J. Wang and X. Ye, A weak Galerkin finite element method for biharmonic equations on polytopal meshes, Numer. Meth. Partial Diff. Eq. 30 (2014), 1003-1029.
[11] L. Mu, J. Wang and X. Ye, Weak Galerkin finite element method for second-order elliptic problems on polytopal meshes, Int. J. Numer. Anal. Model. 12 (2015) 31-53.
[12] L. Mu, J. Wang, X. Ye and S. Zhang, A weak Galerkin finite element method for the Maxwell equations, J. Sci. Comput. 65 (2015), 363-386.
[13] L. Mu, J. Wang, X. Ye and S. Zhao, A new weak Galerkin finite element method for elliptic interface problems, J. Comput. Phy. 325 (2016), 157-173.
[14] S. Shields, J. Li and E.A. Machorro, Weak Galerkin methods for time-dependent Maxwell's equations, Comput. Math. Appl. 74 (2017) 2106-2124.
[15] C. Wang and J. Wang, Discretization of divcurl systems by weak Galerkin finite element methods on polyhedral partitions, J. Sci. Comput. 68 (2016) 1144-1171.
[16] J. Wang, R. Wang, Q. Zhai and R. Zhang, A systematic study on weak Galerkin finite element methods for second order elliptic problems, J. Sci. Comput. 74 (2018), 1369-1396.
[17] J. Wang and X. Ye, A weak Galerkin finite element method for second-order elliptic problems. J. Comput. Appl. Math. 241 (2013), 103-115.
[18] J. Wang and X. Ye, A Weak Galerkin mixed finite element method for second-order elliptic problems, Math. Comp. 83 (2014), 2101-2126.
[19] J. Wang and X. Ye, A weak Galerkin finite element method for the Stokes equations, Adv. Comput. Math. 42 (2016) 155-174.
[20] X. Ye and S. Zhang, A stabilizer-free weak Galerkin finite element method on polytopal meshes, J. Comput. Appl. Math. 372 (2020), 112699, arXiv:1906.06634.
[21] X. Ye, S. Zhang and Y. Zhu, Stabilizer-free weak Galerkin methods for monotone quasilinear elliptic PDEs, Results Appl. Math. https://doi.org/10.1016/j.rinam.2020.100097
[22] X. Ye and S. Zhang, A new weak gradient for the stabilizer-free weak Galerkin finite element method on polytopal meshes, preprint.

Division of Mathematical Sciences, National Science Foundation, Alexandria, VA 22314, U.S.A.
E-mail: jwang@nsf.gov

Department of Mathematics, University of Arkansas at Little Rock, Little Rock, AR 72204, U.S.A.
E-mail: xxye@ualr.edu

Department of Mathematical Sciences, University of Delaware, Newark, DE 19716, U.S.A.
E-mail: szhang@udel.edu